

Microwave spectrum of HSiO in the X^2A' ground electronic state¹

Mitsuaki Izuha^{a,2}, Satoshi Yamamoto^{b,*}, Shuji Saito^c

^aDepartment of Astrophysics, Nagoya University Chikusa-ku, Nagoya 464-01, Japan

^bDepartment of Physics, The University of Tokyo Bunkyo-ku, Tokyo 113, Japan

^cInstitute for Molecular Science, Myodaiji, Okazaki 444, Japan

Received 20 February 1997; accepted 28 February 1997

Abstract

The rotational spectrum of the HSiO radical has been measured in the millimeter- and submillimeter-wave regions. The radical is produced in a d.c. glow discharge plasma of a gaseous mixture of SiH₄ and N₂O. Molecular constants including magnetic hyperfine interaction constants of the hydrogen nucleus are determined accurately from the observed frequencies of 111 a-type R-branch transitions. A portion of quadratic force constants are derived from the centrifugal distortion constants and the inertial defect, and they are used to determine the zero point average structure of HSiO; $r_e(\text{Si-O}) = 1.5326(2)$ Å and $\alpha_e(\text{HSiO}) = 116.8(1)^\circ$, where $r_e(\text{Si-H})$ is assumed to be 1.5066 Å. © 1997 Elsevier Science B.V.

Keywords: Microwave spectrum; HSiO radical; Structure

1. Introduction

Simple transient molecules containing the Si atom have attracted much attention in various fields of chemistry including structural chemistry, reaction dynamics, and interstellar chemistry. Particularly the SiH_nO ($n = 1-4$) molecules are thought to be intermediates in the oxidation process of SiH₄, and play important roles in the chemical vapor deposition process using the SiH₄ discharge plasma. However, spectroscopic studies of these species have been limited so far. The infrared spectra of HSiOH (hydroxysilylene)

and its isotopic species were detected in the Ar matrix by Ismail et al. [1]. Later the H₂SiO (silanone) isomer was also identified in the Ar matrix with infrared spectroscopy [2,3]. Recently, the rotational spectrum of H₂SiO was observed by Bailleux and his collaborators in the discharge plasma of a gaseous mixture of SiH₄, O₂, and Ar [4,5]. An ab initio calculation predicts that H₂SiO is the most stable isomer, although *trans* and *cis* HSiOH isomers are close in energy to H₂SiO [6–9].

On the other hand, only one spectroscopic study has been reported for HSiO and its geometrical isomer. Zee et al. observed the electron spin resonance (ESR) spectrum of HSiO trapped in the Ar and Ne matrices cooled at 4 K [10]. The Fermi contact terms of the hydrogen and ²⁹Si nuclei as well as the *g* factors were determined. They also reported probable identification of HOSi by the same method. Several ab initio calculations were reported for HSiO and HOSi.

* Corresponding author. Tel.: 81 33812 2111, ext. 4197; fax: 81 35802 3325.

¹ Dedicated to Professor Kozo Kuchitsu on the occasion of his 70th birthday.

² Present address: Materials and Devices Research Laboratories, Toshiba Corporation, Toshiba-cho, Saiwai-ku, Kawasaki 210, Japan.

Frenking and Schaefer III [11] obtained the structure, vibrational frequencies, and relative energies for HSiO and its geometrical isomers with the CI calculations using the DZ + P basis set. According to their results, HOSi is the most stable isomer, and there exist two HSiO isomers, A and B, with HSiO angles of 124.3° and 93.0° , respectively. The energy difference between the HOSi isomer and the HSiO isomer (A) is 11 kcal mol^{-1} , and the energy barrier to interconversion is 26 kcal mol^{-1} . Later, Xie and Schaefer III [12] reinvestigated these isomers with the higher level of theory, and found that only one energy minimum exists for the HSiO isomer at the HSiO angle of 120° . Then they estimated the energy of HSiO relative to HOSi to be $11.6 \text{ kcal mol}^{-1}$. Bruna and Grein [13] also studied the energy difference between HSiO and HOSi as well as the electronic excited states of these isomers. Very recently, Yamaguchi et al. [14] carried out a high level calculation on the SiOH–HSiO system, and concluded that the HSiO isomer is less stable than the HOSi isomer by $12.1 \text{ kcal mol}^{-1}$. They also predicted that the activation energy for interconversion from HSiO to HOSi is $24.1 \text{ kcal mol}^{-1}$.

It is of great interest to study the geometrical structures of these isomers and their relative stability in the gas phase in order to make a direct comparison with the above theoretical studies. Microwave spectroscopy is a powerful technique for this purpose because of its high sensitivity and high precision. In this paper, we report microwave spectroscopic detection of the HSiO radical and determination of its molecular structure.

2. Experiment

A source modulation microwave spectrometer combined with a 2-m glow discharge cell was used in the present study. An output from a frequency multiplier driven by a millimeter-wave klystron was used as a microwave source in the frequency range from 180 GHz to 400 GHz. Further details of the spectrometer were described elsewhere [15].

The spectral lines of HSiO were first found during the high sensitivity measurements of H_2CSi [16] in a d.c. glow discharge plasma of a gaseous mixture of SiH_4 and CO. When we were searching for the

12_3-11_3 line of H_2CSi in the 385-GHz region, we found a pair of paramagnetic lines near the H_2CSi line. The separation of the lines, which were thought to be a hyperfine structure of the hydrogen nucleus, is 6 MHz. These lines were not observed by using a mixture of CH_4 and CO, or that of SiH_4 and CH_4 . On the other hand, the lines were weakly observed in a discharge plasma of SiH_4 and O_2 . From these facts, the molecule responsible for the observed lines was thought to have Si, O, and H atoms. The lines were observed as much stronger when we used a mixture of SiH_4 and N_2O . This improvement in production made it possible to search for other related paramagnetic lines in a wide frequency range. As a result, a number of paramagnetic lines were found in the 383–385 GHz region. These lines showed a typical pattern for the a-type R-branch transitions of a nearly prolate asymmetric top radical. A number of paramagnetic lines, which show a similar pattern, were also found in the 344–347 GHz region. Hence, the carrier of these lines is a fairly light molecule with $B + C$ of 39 GHz.

The most probable candidates for the molecule giving the observed lines are HSiO and HOSi. To determine which of these it is, preliminary rotational constants were derived from the observed frequencies; $A = 312\,000 \text{ MHz}$, $B = 19\,886 \text{ MHz}$, $C = 18\,605 \text{ MHz}$. These correspond well to the rotational constants of HSiO calculated from the ab initio structure [12]; $A = 320\,400 \text{ MHz}$, $B = 19\,192 \text{ MHz}$, $C = 18\,107 \text{ MHz}$. On the other hand, the rotational constant, A , of HOSi is expected to be $796\,600 \text{ MHz}$, which is much larger than the observed value. Furthermore the hyperfine splittings due to the hydrogen nucleus are fairly large, suggesting that the unpaired electron is located on the nucleus adjacent to the hydrogen nucleus. From these results, we concluded that the observed lines are due to the HSiO radical in the $^2A'$ electronic ground state.

The optimum condition for production was 20 mTorr of SiH_4 and 6 mTorr of N_2O with the discharge current of about 20 mA. The cell was kept at -150°C by slowly flowing liquid nitrogen in a copper jacket attached to the cell. Finally we measured the frequencies of 111 lines listed in Table 1. Each frequency was determined from five pairs of forward and reverse frequency scans covering the line frequency. An example of the observed spectrum is shown in Fig. 1.

Table 1
Observed and calculated transition frequencies of HSiO (MHz)

N_{K_a, K_c}	$N_{K_a', K_c'}$	J'	J''	F'	F''	ν_{obs}	$\Delta\nu$
5 ₀₅	4 ₀₄	9/2	7/2	4	3	192386.839	0.006
5 ₀₅	4 ₀₄	9/2	7/2	5	4	192374.264	-0.005
5 ₀₅	4 ₀₄	11/2	9/2	5	4	192358.354	0.013
5 ₀₅	4 ₀₄	11/2	9/2	6	5	192345.793	0.024
5 ₁₅	4 ₁₄	9/2	7/2	4	3	189383.843	0.010
5 ₁₅	4 ₁₄	9/2	7/2	5	4	189333.380	0.007
5 ₁₅	4 ₁₄	11/2	9/2	5	4	189161.396	-0.007
5 ₁₅	4 ₁₄	11/2	9/2	6	5	189110.984	0.000
5 ₁₄	4 ₁₃	9/2	7/2	4	3	195713.116	-0.005
5 ₁₄	4 ₁₃	9/2	7/2	5	4	195700.097	0.003
5 ₁₄	4 ₁₃	11/2	9/2	5	4	195557.274	0.025
5 ₁₄	4 ₁₃	11/2	9/2	6	5	195544.238	0.027
6 ₀₆	5 ₀₅	11/2	9/2	5	4	230807.622	-0.003
6 ₀₆	5 ₀₅	11/2	9/2	6	5	230796.302	0.001
6 ₀₆	5 ₀₅	13/2	11/2	7	6	230766.195	-0.009
6 ₁₆	5 ₁₅	11/2	9/2	5	4	227175.998	-0.004
6 ₁₆	5 ₁₅	11/2	9/2	6	5	227102.903	0.011
6 ₁₆	5 ₁₅	13/2	11/2	6	5	227033.628	-0.020
6 ₁₆	5 ₁₅	13/2	11/2	7	6	226960.553	-0.007
6 ₁₅	5 ₁₄	11/2	9/2	5	4	234779.882	-0.002
6 ₁₅	5 ₁₄	11/2	9/2	6	5	234769.909	-0.018
6 ₁₅	5 ₁₄	13/2	11/2	6	5	234683.426	0.008
6 ₁₅	5 ₁₄	13/2	11/2	7	6	234673.367	-0.001
6 ₂₅	5 ₂₄	11/2	9/2	5	4	231168.667	0.024
6 ₂₅	5 ₂₄	11/2	9/2	6	5	231161.674	0.002
6 ₂₅	5 ₂₄	13/2	11/2	7	6	230623.456	0.021
6 ₂₄	5 ₂₃	11/2	9/2	5	4	231310.739	-0.025
6 ₂₄	5 ₂₃	11/2	9/2	6	5	231303.833	-0.020
6 ₂₄	5 ₂₃	13/2	11/2	7	6	230771.152	0.009
7 ₀₇	6 ₀₆	13/2	11/2	6	5	269196.490	0.007
7 ₀₇	6 ₀₆	13/2	11/2	7	6	269187.050	0.004
7 ₀₇	6 ₀₆	15/2	13/2	7	6	269167.683	-0.005
7 ₀₇	6 ₀₆	15/2	13/2	8	7	269158.136	-0.002
7 ₁₇	6 ₁₆	13/2	11/2	6	5	264974.938	0.023
7 ₁₇	6 ₁₆	15/2	13/2	8	7	264793.007	-0.017
7 ₁₆	6 ₁₅	13/2	11/2	6	5	273852.446	-0.015
7 ₁₆	6 ₁₅	13/2	11/2	7	6	273859.382	-0.018
7 ₁₆	6 ₁₅	15/2	13/2	7	6	273926.917	-0.002
7 ₁₆	6 ₁₅	15/2	13/2	8	7	273914.596	-0.004
7 ₂₆	6 ₂₅	13/2	11/2	6	5	269539.454	0.005
7 ₂₆	6 ₂₅	13/2	11/2	7	6	269533.024	0.009
7 ₂₆	6 ₂₅	15/2	13/2	7	6	269139.518	0.020
7 ₂₆	6 ₂₅	15/2	13/2	8	7	269133.097	0.020
7 ₂₅	6 ₂₄	13/2	11/2	6	5	269767.421	-0.021
7 ₂₅	6 ₂₄	13/2	11/2	7	6	269761.122	-0.015
7 ₂₅	6 ₂₄	15/2	13/2	7	6	269374.981	0.000
7 ₂₅	6 ₂₄	15/2	13/2	8	7	269368.702	-0.012
9 ₀₉	8 ₀₈	17/2	15/2	8	7	346088.325	0.001
9 ₀₉	8 ₀₈	17/2	15/2	9	8	346025.860	0.006
9 ₀₉	8 ₀₈	19/2	17/2	9	8	345881.607	0.005
9 ₀₉	8 ₀₈	19/2	17/2	10	9	345837.945	-0.041
9 ₁₉	8 ₁₈	17/2	15/2	8	7	340559.654	0.020
9 ₁₉	8 ₁₈	17/2	15/2	9	8	340530.021	0.009

Table 1 Continued

N_{K_u, K_c}^+	N_{K_u, K_c}^-	J'	J''	F'	F''	ν_{obs}	$\Delta\nu$
9 ₁₉	8 ₁₈	19/2	17/2	9	8	340442.774	0.023
9 ₁₉	8 ₁₈	19/2	17/2	10	9	340413.096	-0.034
9 ₁₈	8 ₁₇	17/2	15/2	8	7	351980.555	0.005
9 ₁₈	8 ₁₇	17/2	15/2	9	8	351975.401	0.010
9 ₁₈	8 ₁₇	19/2	17/2	9	8	351950.785	0.000
9 ₁₈	8 ₁₇	19/2	17/2	10	9	351945.943	0.006
9 ₂₈	8 ₂₇	17/2	15/2	8	7	346337.410	-0.002
9 ₂₈	8 ₂₇	17/2	15/2	9	8	346330.979	0.008
9 ₂₈	8 ₂₇	19/2	17/2	9	8	346084.790	0.000
9 ₂₈	8 ₂₇	19/2	17/2	10	9	346078.338	-0.016
9 ₂₇	8 ₂₆	17/2	15/2	8	7	346827.173	-0.008
9 ₂₇	8 ₂₆	17/2	15/2	9	8	346821.198	0.010
9 ₂₇	8 ₂₆	19/2	17/2	9	8	346586.779	-0.006
9 ₂₇	8 ₂₆	19/2	17/2	10	9	346580.791	-0.038
9 ₃₇	8 ₃₆	17/2	15/2	9	8	346508.689	0.057
9 ₃₇	8 ₃₆	19/2	17/2	10	9	345980.307	-0.014
9 ₃₆	8 ₃₅	17/2	15/2	8	7	346515.412	-0.077
9 ₃₆	8 ₃₅	19/2	17/2	9	8	345987.273	-0.053
9 ₄	8 ₄	17/2	15/2	8	7	346535.105	0.003
9 ₄	8 ₄	17/2	15/2	9	8	346532.822	-0.013
9 ₄	8 ₄	19/2	17/2	9	8	345615.342	0.018
9 ₄	8 ₄	19/2	17/2	10	9	345613.051	0.003
9 ₅	8 ₅	17/2	15/2	8	7	346590.802	0.036
9 ₅	8 ₅	17/2	15/2	9	8	346588.857	-0.012
9 ₅	8 ₅	19/2	17/2	9	8	345161.872	0.011
9 ₅	8 ₅	19/2	17/2	10	9	345159.885	-0.009
10 ₀₁₀	9 ₀₉	19/2	17/2	9	8	384160.437	0.022
10 ₀₁₀	9 ₀₉	19/2	17/2	10	9	384153.474	0.007
10 ₀₁₀	9 ₀₉	21/2	19/2	11	10	384116.788	-0.028
10 ₁₁₀	9 ₁₉	19/2	17/2	9	8	378337.313	-0.011
10 ₁₁₀	9 ₁₉	19/2	17/2	10	9	378318.122	-0.013
10 ₁₁₀	9 ₁₉	21/2	19/2	10	9	378219.873	0.029
10 ₁₁₀	9 ₁₉	21/2	19/2	11	10	378200.648	-0.004
10 ₁₉	9 ₁₈	19/2	17/2	9	8	391027.225	0.020
10 ₁₉	9 ₁₈	19/2	17/2	10	9	391022.303	0.014
10 ₁₉	9 ₁₈	21/2	19/2	10	9	390999.648	-0.015
10 ₁₉	9 ₁₈	21/2	19/2	11	10	390994.786	-0.017
10 ₂₉	9 ₂₈	19/2	17/2	9	8	384739.941	0.007
10 ₂₉	9 ₂₈	19/2	17/2	10	9	384733.061	-0.021
10 ₂₉	9 ₂₈	21/2	19/2	10	9	384529.583	0.002
10 ₂₉	9 ₂₈	21/2	19/2	11	10	384522.714	-0.017
10 ₂₈	9 ₂₇	19/2	17/2	9	8	385413.528	0.019
10 ₂₈	9 ₂₇	19/2	17/2	10	9	385407.435	0.009
10 ₂₈	9 ₂₇	21/2	19/2	10	9	385218.089	0.024
10 ₂₈	9 ₂₇	21/2	19/2	11	10	385212.026	0.007
10 ₃₈	9 ₃₇	19/2	17/2	10	9	384918.959	0.074
10 ₃₈	9 ₃₇	21/2	19/2	10	9	384490.079	0.049
10 ₃₈	9 ₃₇	21/2	19/2	11	10	384487.166	0.041
10 ₃₇	9 ₃₆	19/2	17/2	9	8	384928.259	-0.005
10 ₃₇	9 ₃₆	19/2	17/2	10	9	384925.304	-0.043
10 ₃₇	9 ₃₆	21/2	19/2	10	9	384496.716	-0.023
10 ₃₇	9 ₃₆	21/2	19/2	11	10	384493.789	-0.048
10 ₄	9 ₄	19/2	17/2	9	8	384871.584	0.043

Table 1 Continued

$N_{K_a, K}$	$N_{K_a, K'}$	J'	J''	F'	F''	ν_{obs}	$\Delta\nu$
10 ₄	9 ₄	19/2	17/2	10	9	384869.488	-0.020
10 ₃	9 ₃	19/2	17/2	9	8	384837.080	0.004
10 ₅	9 ₅	19/2	17/2	10	9	384835.376	-0.034
10 ₅	9 ₅	21/2	19/2	10	9	383687.174	0.027
10 ₅	9 ₅	21/2	19/2	11	10	383685.421	-0.029

3. Analysis

The observed transition frequencies were analyzed by using a standard Hamiltonian for an asymmetric top radical including magnetic hyperfine interactions [17]:

$$H = H_{\text{rot}} + H_{\text{cd}} + H_{\text{sr}} + H_{\text{srd}} + H_{\text{hf}} \quad (1)$$

where H_{rot} represents the rotational Hamiltonian, H_{cd} the centrifugal distortion terms, H_{sr} the spin rotation interaction terms, H_{srd} the centrifugal distortion correction for H_{sr} , and H_{hf} the hyperfine interaction terms of the hydrogen nucleus. Since the hydrogen nucleus has a nuclear spin of $I = 1/2$, the following coupling scheme of the angular momenta was employed; $J = N + S$ and $F = J + I$, where N and S denote the angular momentum of an end-over-end rotation of the molecule and that of the electron spin, respectively. A Hamiltonian matrix involves all the off-diagonal interactions with $\Delta N = 0, 1$, and 2 due to the spin rotation interaction and the hyperfine interaction. The matrix for each F is numerically diagonalized to obtain the energy levels.

Rotational constants, centrifugal distortion constants, spin rotation interaction constants and their centrifugal distortion corrections, and the magnetic hyperfine interaction constants were determined by a least-squares analysis from the observed transition frequencies with K_a up to 5. The frequency of an unresolved K doublet line was compared with a calculated frequency averaged for the frequencies of the component lines. Although we only observed the a-type R-branch transitions, the D_K constant was determined in the fit. In fact, the standard deviation of the fit was much larger, when we assume the D_K constant of a similar sized molecule, HSO (27.2 MHz) [18,19]. In this analysis we included the higher order centrifugal distortion correction for the spin-rotation interaction, 6H_K , which depends on K_a^6 .

In the course of the analysis, we noticed an anomaly of the spin doubling in the 9₀₉–8₀₈ and 7₁₆–6₁₅ transitions. This can be explained by an effect of the off-diagonal term of the spin rotation interaction, $\epsilon_{ab} + \epsilon_{ba}$, which has a matrix element between the N_{0N} , $J = N - 1/2$ and $(N - 1)_{1N-2}$, $J = N - 1/2$ levels [17,20]. In the case of HSiO, these levels become close in energy to each other at about $N = 8$. Therefore 8₀₈, the $J = 15/2$ and 7₁₆, $J = 15/2$ levels are most influenced by this term. Because of the heavy mixing of the wave functions in both levels, the off-diagonal term in the dipolar hyperfine interaction tensor, T_{ab} , was also determined with sufficient accuracy. Furthermore, the energy difference between the $K_a = 0$ and $K_a = 1$ levels is well determined because of the interaction. This is an important reason why the D_K constant is determined in the present study.

The result of the least-squares fit is shown in Table 1, and the molecular constants determined are summarized in Table 2. The standard deviation of the fit was 24 kHz, which is almost comparable to the frequency measurement error.

4. Results and discussion

In the present study, the HSiO radical was identified in the gas phase for the first time, although the ab initio calculations suggest that the HOSi isomer is more stable than the HSiO isomer [11–14]. According to the ab initio calculation [14], the dipole moment of HOSi is smaller than that of HSiO, which may be a reason why we first detected the HSiO isomer. A search for the HOSi spectrum is now being carried out. In the following sections, we discuss the molecular structure and intramolecular potential functions of HSiO.

Table 2

Molecular constants of the HSiO radical (MHz)^a

<i>A</i>	312105(20)	ϵ_{aa}	4604.55(75)
<i>B</i>	19887.009(56)	ϵ_{bb}	63.197(61)
<i>C</i>	18605.416(55)	ϵ_{cc}	−139.685(47)
Δ_N	0.0247506(167)	$(\epsilon_{ab} + \epsilon_{ba})/2^b$	262.797(197)
Δ_{NK}	1.30194(48)	$^*\Delta_{NK}$	−0.0918(126)
Δ_K	146.8(168)	$^*\Delta_K$	−7.015(140)
δ_N	0.0021953(145)	*H_K	0.0188(41)
δ_K	1.283(28)	α_F	451.32(45)
H_{NK}	0.0000184(25)	T_{aa}	1.69(83)
H_{KN}	−0.0007761(112)	T_{bb}	2.38(149)
		T_{ab}	3.99(50)

^aNumbers in parentheses represent three standard deviations in units of the last significant digits.^bRelative sign between $(\epsilon_{ab} + \epsilon_{ba})/2$ and T_{ab} is correct.

4.1. Centrifugal distortion constants and harmonic force field

All the quartic centrifugal distortion constants, Δ_N , Δ_{NK} , Δ_K , δ_N , and δ_K , were determined in the present study. When they are compared with the corresponding constants for a similar sized molecule, HSO [18,19], the Δ_{NK} , Δ_K , and δ_K constants of HSiO are significantly larger than those of HSO ($\Delta_{NK} = 0.8960$ MHz, $\Delta_K = 27.2$ MHz, and $\delta_K = 0.89$ MHz). On the other hand, the Δ_N and δ_N constants of HSiO are comparable to or even smaller than those of HSO ($\Delta_N = 0.03070$ MHz and $\delta_N = 0.00193$ MHz). Furthermore, the inertial defect derived from the observed rotational constants is $0.1312(1) \text{ u}\text{\AA}^2$, which is larger than that of HSO ($0.0754 \text{ u}\text{\AA}^2$) [18]. These results

indicate that the vibrational frequency for at least one mode in HSiO is significantly lower than that in HSO. The ab initio calculation [14] predicts that the HSiO bending mode has a low vibrational frequency (723 cm^{-1}) in comparison with the bending frequency for HSO (1063 cm^{-1}) [21,22]. In order to confirm this, we derived the harmonic force constants from the centrifugal distortion constants and the inertial defect.

A nonlinear XYZ type molecule like HSiO has six quadratic force constants. When we take $\Delta R(\text{Si}-\text{O})$, $\Delta r(\text{H}-\text{Si})$, and $\Delta\alpha(\text{HSiO})$ as internal coordinates, S_1 , S_2 , and S_3 , respectively, they are F_{11} , F_{22} , F_{33} , F_{12} , F_{13} , and F_{23} . We developed a computer program to determine these constants from the centrifugal distortion constants and the inertial defect by a least-squares method. This program was successfully applied to determine the harmonic force field of the HSS radical [23]. Since we have only six independent data in the case of HSiO, only four force constants, F_{11} , F_{33} , F_{13} , and F_{23} , were determined for HSiO, as listed in Table 3. The result of the fit is shown in Table 4. In

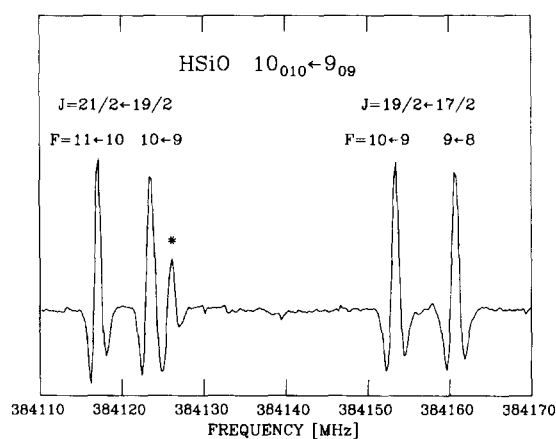


Fig. 1. An example of the rotational spectrum of HSiO. The line with an asterisk is a diamagnetic line of an unknown species.

Table 3

Harmonic force field of the HSiO radical^a

F_{11}	8.409(154)	F_{12}	0.0(fixed)
F_{22}	2.54(fixed) ^b	F_{13}	0.063(20)
F_{33}	0.1606(164)	F_{23}	0.109(55)

^aIn $\text{mdyn } \text{\AA}^{-1}$. The internal coordinates are as follows: $S_1 = \Delta r(\text{Si}-\text{O})$; $S_2 = \Delta r(\text{Si}-\text{H})$; $S_3 = \Delta\alpha(\text{HSiO})$. Numbers in parentheses represent one standard deviation in units of the last significant digits.

^bAdjusted to reproduce the ν_1 vibrational frequency, 2107 cm^{-1} , estimated by the ab initio calculation [14].

Table 4

Observed calculated centrifugal distortion constants inertial defect of the HSiO radical

	Obs.	Calc.
Δ_N (MHz)	0.0247506	0.0247312
Δ_{NK} (MHz)	1.30194	1.30315
Δ_K (MHz)	146.8	150.5
δ_N (MHz)	0.0021953	0.0022962
δ_K (MHz)	1.283	1.123
Δ_{II}^a (uA ²)	0.1312	0.1285
ω_1 (cm ⁻¹)	—	2107
ω_2 (cm ⁻¹)	—	1180
ω_3 (cm ⁻¹)	—	555

^aInertial defect.

this analysis, the F_{22} constant was fixed to the value which reproduces the vibrational frequency of the Si–H stretching mode (2107 cm⁻¹) calculated by the ab initio method [14], whereas the F_{12} constant was set to zero. These two force constants are rather insensitive to the centrifugal distortion constants and inertial defect, and hence, the above assumptions are justified. By using the force constants determined, the vibrational frequencies for the Si–O stretching mode and the HSiO bending mode are evaluated to be 1180 cm⁻¹ and 555 cm⁻¹, respectively (Table 4). The bending mode in HSiO has a much lower frequency than that in HSO [21,22].

The vibrational frequencies of the HSiO bending and the Si–O stretching modes determined in the present study are lower than the ab initio values [14], 723 cm⁻¹ and 1272 cm⁻¹, respectively. Particularly the difference is significant for the HSiO bending motion. This may indicate an effect of anharmonicity of the HSiO bending mode, which is a promoting mode to

isomerization to SiOH [11–14]. These vibrational frequencies would be useful in the future search for the infrared spectrum of HSiO.

4.2. Molecular structure

The molecular structure of HSiO is determined from the rotational constants. The r_0 structure directly derived from the observed rotational constants suffers from the vibration–rotation interaction, and hence, the structural parameters have a large uncertainty due to the inertial defect. In order to avoid this difficulty, we determined the zero point average structure (r_e) in the present study.

The rotational constant which corresponds to the r_e structure is related to the observed rotational constant as follows [24,25]:

$$B_e = B_0 + (1/2)\Sigma\alpha^B(\text{harm}) \quad (2)$$

where $\alpha^B(\text{harm})$ represents the harmonic part of the vibration–rotation constants, which can be calculated from the harmonic force constants. Similar relations hold for A_e and C_e . We evaluated A_e , B_e , and C_e from the observed rotational constants to be 302 928 MHz, 19 803 MHz, and 18 585 MHz, respectively, where a small contribution of the second term in Eq. (2) is calculated with the aid of the harmonic force field determined in the present study. The $r_e(\text{Si–O})$ and $\alpha_e(\text{HSiO})$ have been determined from the corrected rotational constants by a least-squares method to be 1.5326(2) Å and 116.8(1)°, respectively. In this calculation, $r_e(\text{Si–H})$ is assumed to be 1.5066 Å, which is evaluated from the ab initio equilibrium distance, 1.4971 Å [14], and a small correction between the r_e distance and the equilibrium (r_e) distance, 0.0095 Å.

Table 5

Molecular structure of the HSiO radical^a

	r_e^b	r_e^c	Ab initio ^d	Ab initio ^e
$r(\text{Si–H})$ (Å)	1.5066(fixed)	1.4971(fixed)	1.4971	1.503
$r(\text{Si–O})$ (Å)	1.5326(2)	1.5286(2)	1.5085	1.516
$\alpha(\text{HSiO})$ (°)	116.8(1)	116.8(1)	122.37	121.8

^aNumbers in parentheses represent three standard deviations in units of the last significant digits.^bPresent study.^cPresent study. The equilibrium distance of Si–O is evaluated by use of Eq. (3), where the a constant for the SiO molecule (1.970 Å⁻¹) is employed [25]. The equilibrium angle of HSiO is assumed to be the same as $\alpha_e(\text{HSiO})$.^dYamaguchi et al. [14]. TZ2P(f.d) + diff CISD level of theory.^eXie and Schaefer [12]. TZ2P CISD level of theory.

The latter correction was calculated by using the following approximate relation [25];

$$r_z - r_c = (3/2)a(\Delta r^2) - (\langle \Delta x^2 \rangle + \langle \Delta y^2 \rangle) / (2r_c) \quad (3)$$

where a represents the third-order anharmonic constant and the Δx and Δy denote the displacements of the local Cartesian coordinates perpendicular to the bond direction. As for the a constant, we employed the corresponding value for the SiH radical (1.530 Å⁻¹), and the vibrational averages of the square displacements were calculated from the harmonic force field obtained above [25]. It should be noted that $r_z(\text{Si-O})$ and $\alpha_z(\text{HSiO})$ are rather insensitive to the assumed value for $r_z(\text{Si-H})$; when $r_z(\text{Si-H})$ increases by 0.01 Å from the assumed value, $r_z(\text{Si-O})$ and $\alpha_z(\text{HSiO})$ change by -0.001 Å and 0.7° , respectively.

The determined structure is compared with that derived from the ab initio calculations in Table 5. For a detailed comparison, we derived the $r_c(\text{Si-O})$ distance by using Eq. (3), since the structure reported in the ab initio studies is the equilibrium one. The SiO distance in HSiO is slightly longer than that derived from ab initio calculations as shown in Table 5. It is significantly shorter than the Si-O single bond distance in *cis*-HSiOH, 1.658 Å [8], and is slightly longer than the Si=O double bond in H₂SiO, 1.515 Å [5]. Therefore the Si-O bond in HSiO seems to have a double bond character. The HSiO angle obtained in this study is smaller than those reported in the ab initio calculations (Table 5). Even if we consider a systematic error caused by the assumption of $r_z(\text{Si-H})$, this difference seems to be significant. Nevertheless, it is close to 120°, which indicates the sp² hybrid orbitals in the Si atom. This is consistent with the double bond nature of the SiO bond.

4.3. Fine and hyperfine interaction constants

The Fermi contact term, a_F , for the hydrogen nucleus takes a large positive value, indicating that the unpaired electron occupies the molecular orbital extending within the molecular plane. Moreover, the spin rotation interaction constant, ϵ_{cc} , takes a negative value. These two results undoubtedly indicate that the ground electronic state of HSiO is ²A', which is consistent with the results of the ab initio calculations [11–14].

The Fermi contact term determined in the present

study (451.30 MHz) is in good agreement with that reported from the ESR study (450 MHz) [10]. The spin density on the hydrogen nucleus is estimated to be 31% by comparing the observed Fermi contact term with the corresponding atomic value [26]. In the present study, the off-diagonal term of the dipolar interaction tensor, T_{ab} , has been determined. We can then determine the principal values of the dipolar interaction tensor; $T_{xx} = 6.0(6)$ MHz, $T_{yy} = -2.0(13)$ MHz, and $T_{zz} = -4.1(15)$ MHz, where Z axis is taken to be perpendicular to the molecular plane. The angle between the X axis and the a axis is determined to be $48(6)^\circ$. The numbers in parentheses represent three times the standard deviations in units of the last significant digits. Since the angle between the H-Si bond and the a axis is 59° , the direction of the tensor (X axis) is almost parallel to the H-Si bond. This result is consistent with that reported for HSiS [27].

The spin-rotation interaction constant, ϵ_{aa} is approximately related to the energy difference between the ground and first A'' electronic state, ΔE as

$$\epsilon_{aa} = 4A_{so}/\Delta E \quad (4)$$

where A_{so} is an off-diagonal spin-orbit interaction constant of the HSiO. The energy difference is estimated by using Eq. (4) to be 40 000 cm⁻¹, where the spin-orbit interaction constant of the Si atom (148.9 cm⁻¹) [28] is employed as A_{so} . It should be noted that this value is fairly high compared with the excitation energy of the first A'' state predicted by the ab initio calculation (20 900 cm⁻¹) [13].

Acknowledgements

SY thanks Sumitomo Foundation for financial support. This study is supported by Grant-in-Aid from the Ministry of Education, Science, and Culture (Nos. 04233107, 05453020, and 07CE2001).

References

- [1] Z.K. Ismail, R.H. Hague, L. Fredin, J.W. Kauffman, J.L. Margrave, *J. Chem. Phys.* 77 (1982) 1617.
- [2] R. Withnall, L. Andrews, *J. Am. Chem. Soc.* 107 (1985) 2567.
- [3] R. Withnall, L. Andrews, *J. Phys. Chem.* 89 (1985) 3261.

- [4] S. Bailleux, M. Bogey, C. Demuynck, J.-L. Destombes, A. Walters, *J. Chem. Phys.* 101 (1994) 2729.
- [5] M. Bogey, B. Delcroix, A. Walters, J.-C. Guillemin, *J. Mol. Spectrosc.* 175 (1996) 421.
- [6] T. Kudo, S. Nagase, *J. Phys. Chem.* 88 (1984) 2833.
- [7] C.L. Darling, H.B. Schlegel, *J. Phys. Chem.* 97 (1993) 8207.
- [8] B. Ma, H.F. Schaefer III, *J. Chem. Phys.* 101 (1994) 2734.
- [9] B. Ma, N.L. Allinger, H.F. Schaefer III, *J. Chem. Phys.* 105 (1996) 5731.
- [10] R.J. van Zee, R.F. Ferrante, W. Weltner Jr., *J. Chem. Phys.* 83 (1985) 6181.
- [11] G. Frenking, H.F. Schaefer III, *J. Chem. Phys.* 82 (1985) 4585.
- [12] Y. Xie, H.F. Schaefer III, *J. Chem. Phys.* 93 (1990) 1196.
- [13] P.J. Bruna, F. Grein, *Mol. Phys.* 63 (1988) 329.
- [14] Y. Yamaguchi, Y. Xie, S.-J. Kim, H.F. Schaefer III, *J. Chem. Phys.* 105 (1996) 1951.
- [15] S. Yamamoto, S. Saito, *J. Chem. Phys.* 89 (1988) 1936.
- [16] M. Izuha, S. Yamamoto, S. Saito, *J. Chem. Phys.* 105 (1996) 4923.
- [17] I.C. Bowater, J.M. Brown, A. Carrington, *Proc. R. Soc. Lond. A* 333 (1973) 265.
- [18] Y. Endo, S. Saito, E. Hirota, *J. Chem. Phys.* 75 (1981) 4379.
- [19] M. Kakimoto, S. Saito, E. Hirota, *J. Mol. Spectrosc.* 80 (1980) 334.
- [20] S. Saito, *J. Mol. Spectrosc.* 65 (1977) 229.
- [21] U. Schurath, M. Weber, K.H. Becker, *J. Chem. Phys.* 67 (1977) 110.
- [22] N. Ohashi, M. Kakimoto, S. Saito, E. Hirota, *J. Mol. Spectrosc.* 84 (1980) 204.
- [23] S. Yamamoto, S. Saito, *Can. J. Phys.* 72 (1994) 954.
- [24] M. Toyama, T. Oka, Y. Morino, *J. Mol. Spectrosc.* 13 (1964) 193.
- [25] K. Kuchitsu, M. Nakata, S. Yamamoto, in: I. Hargittai, M. Hargittai (Eds.), *Stereochemical Applications of Gas-Phase Electron Diffraction. Part A. The Electron Diffraction Technique*, VCH, New York, 1988, p. 227.
- [26] C.H. Townes, A.L. Schawlow, *Microwave Spectroscopy*, McGraw-Hill, New York, 1955.
- [27] F.X. Brown, S. Yamamoto, S. Saito, *J. Mol. Struct.*, in press.
- [28] H. Lefebvre-Brion, R.W. Field, *Perturbation in the Spectra of Diatomic Molecules*, Academic Press, New York, 1986, p. 214.